

Chapter 3

Receiver Function Method

3.1 Introduction

Characterisation of the detailed structure of the crust and the upper mantle is a continuous goal of geophysical studies, in which the receiver function method is a relatively new powerful technique in obtaining information about discontinuities in the crust and the upper mantle beneath three component seismic stations.

In Receiver function technique the teleseismic body waveforms is used to image the crustal structures underneath isolated seismic stations. These waveforms contain informations related to the source time function, propagation effect through the mantle and local structures underneath the recording site. The resulting receiver function is obtained by removing the effects of source and mantle path effects.

The basic aspect of this method is that part of the P waves signals from distant events incident to a discontinuity in the crust or upper mantle will be converted to S waves (Ps), that arrive at the station within the P wave coda directly after the direct P wave (Fig. 3.1A). Basically, the S waves travel slower than the P waves, so, a direct measure of the depth of the discontinuity is calculated by the time difference in the arrival of the direct P wave and the converted phase (Ps), provided the velocity model is known.

The resulting Ps conversions which are sensitive to shear velocity contrasts have much stronger amplitude on the horizontal component than on the vertical. These Ps converted phases are identified on the Q-component seismogram, termed as the receiver functions. In addition to the direct Ps converted phases, the multiples resulting from the discontinuity and free surface (Fig.3.1A), are also seen on the receiver function traces (Fig 3.1B).

Fig. 3.1A shows two types of multiples, PpPs and PpSs following the direct Ps phase and (Fig 3.1B) shows the corresponding receiver function trace. It is also clear from the Fig. 3.1B that the converted Ps as well as the first multiple (PpPs) have a positive polarity, while the second multiple (PpSs) has a negative polarity.

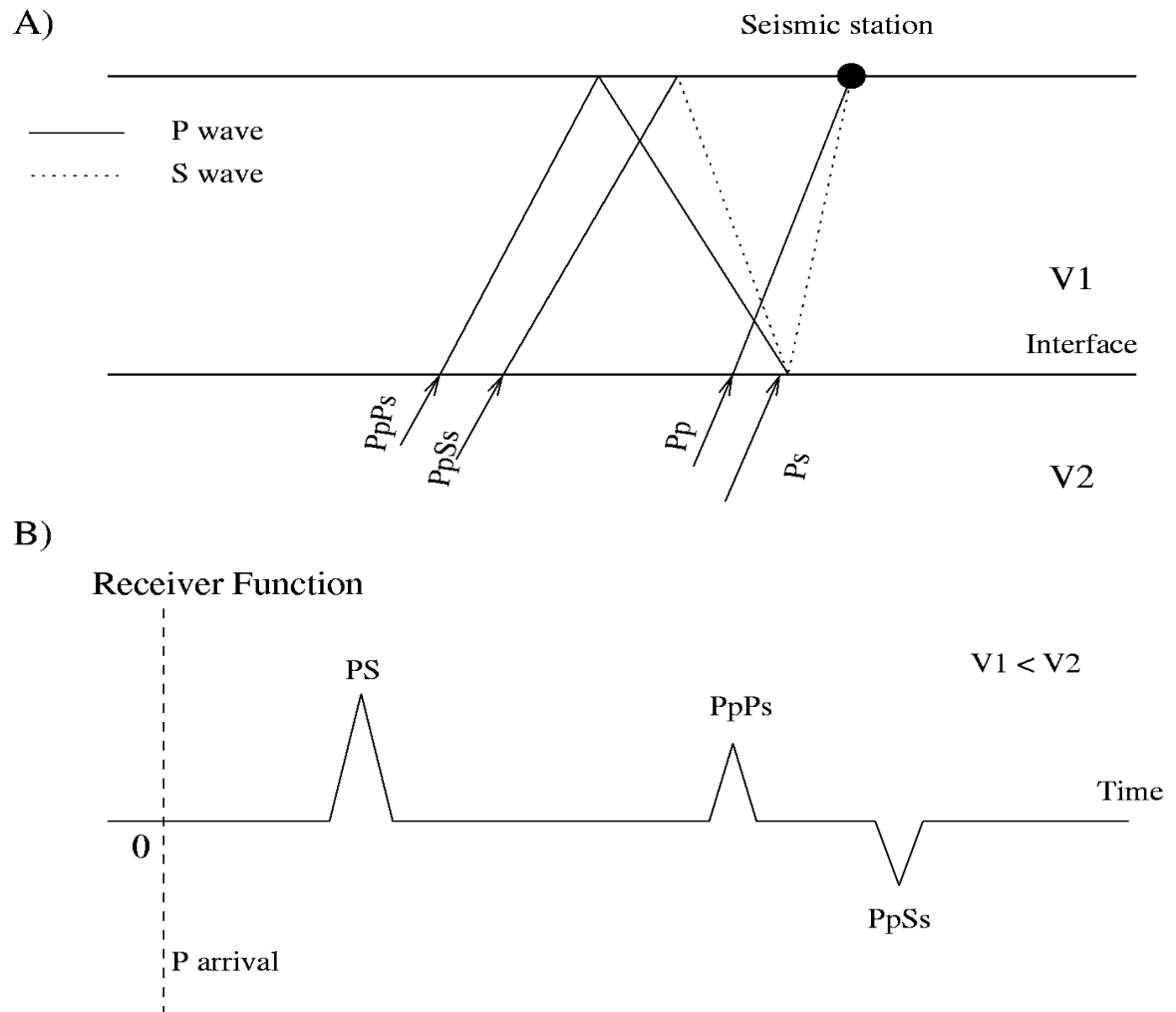


Figure 3.1: A) Diagram showing the major Ps converted phases for a layer over a half space model. B) Simplified Q-component receiver function corresponding to the model in A) showing the direct P and the Ps conversions from the Moho and its multiples.

In this chapter, a brief discussion will be presented about analysing Ps converted waves necessary to isolate the response of the crust and the upper mantle beneath a three component seismic station from the observed teleseismic P waveforms.

3.2 Receiver Function Processing

3.2.1 Restitution

Different instruments types must be considered for the detection and analysis of teleseismic waves. Our temporary network (see Chapter 4) consists mainly of broadband (Guralp 3T, Guralp 40T, STS2) and shortperiod (1-Hz, Mark L4) seismometers, which are quite different in their frequency responses. For receiver function studies, useful teleseismic waves have frequencies in the range of 0.1 Hz to 1 Hz.

A teleseismic earthquake of magnitude 6.2, recorded at two neighboring stations (ID06 and ID27), is illustrated in Fig. 3.2 . The first 6 traces are the original earthquake records. The waveforms for these two stations are quite different because of the different instrument responses.

In the first step to isolate the receiver effects of the seismograms recorded at different instruments, the respective instrument responses has to be deconvolved from the receiver functions. The frequency response of the the broadband seismometers are flat in the useful range for receiver function analysis. In case of short period seismograms the frequency responses are broaden by the application of restitution. The last 6 traces in Fig. 3.2 are the restituted traces proportional to ground displacement for both the broadband and the shortperiod instruments which have similar waveforms.

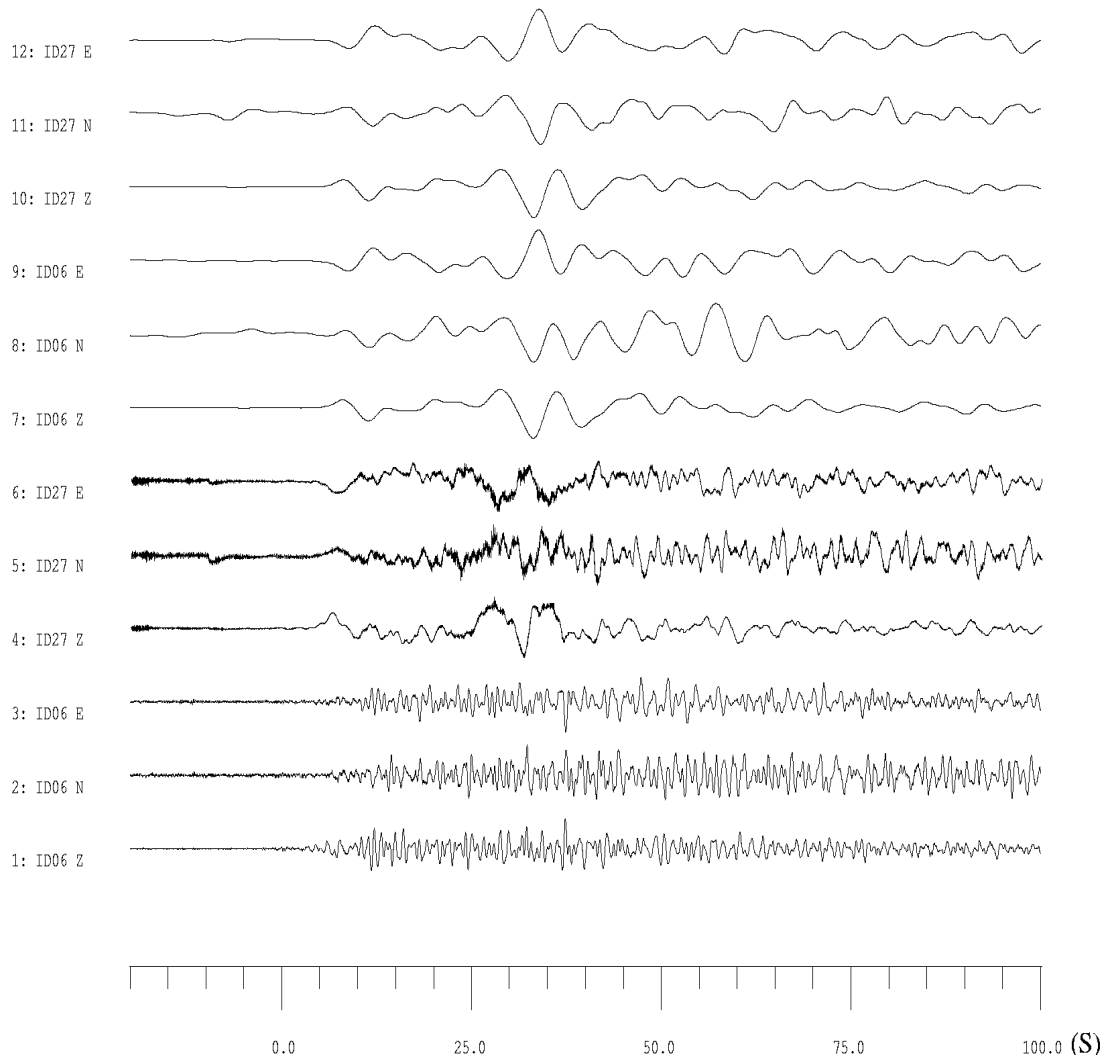


Figure 3.2: A data example to show the restitution step. The first 6 traces (1-6) are the original recordings of the earthquake on 13 February 2001 recorded at two neighboring stations: broadband (ID27) and shortperiod (ID06) (see Fig. 4.1 for the location). The broadband record is proportional to ground velocity. The restitution step consists in this case simply is the integration to obtain ground displacement. The waveforms are quite different because of the different instrument responses. The upper 6 traces (7-12) are the new traces after restitution step. The waveforms of the two stations are now similar.

3.2.2 Rotation

In order to isolate the converted S phases from the direct P wave, each seismogram is rotated from the original Z, NS and EW components of the P wave into the L, Q and T coordinate system (Fig. 3.3). The L-component points in the direction of the direct P wave, while the Q-component is perpendicular to L-component. The T component is perpendicular to both L and Q components. The L, Q and T components contain mainly P-energy, SV-energy and SH-energy, respectively.

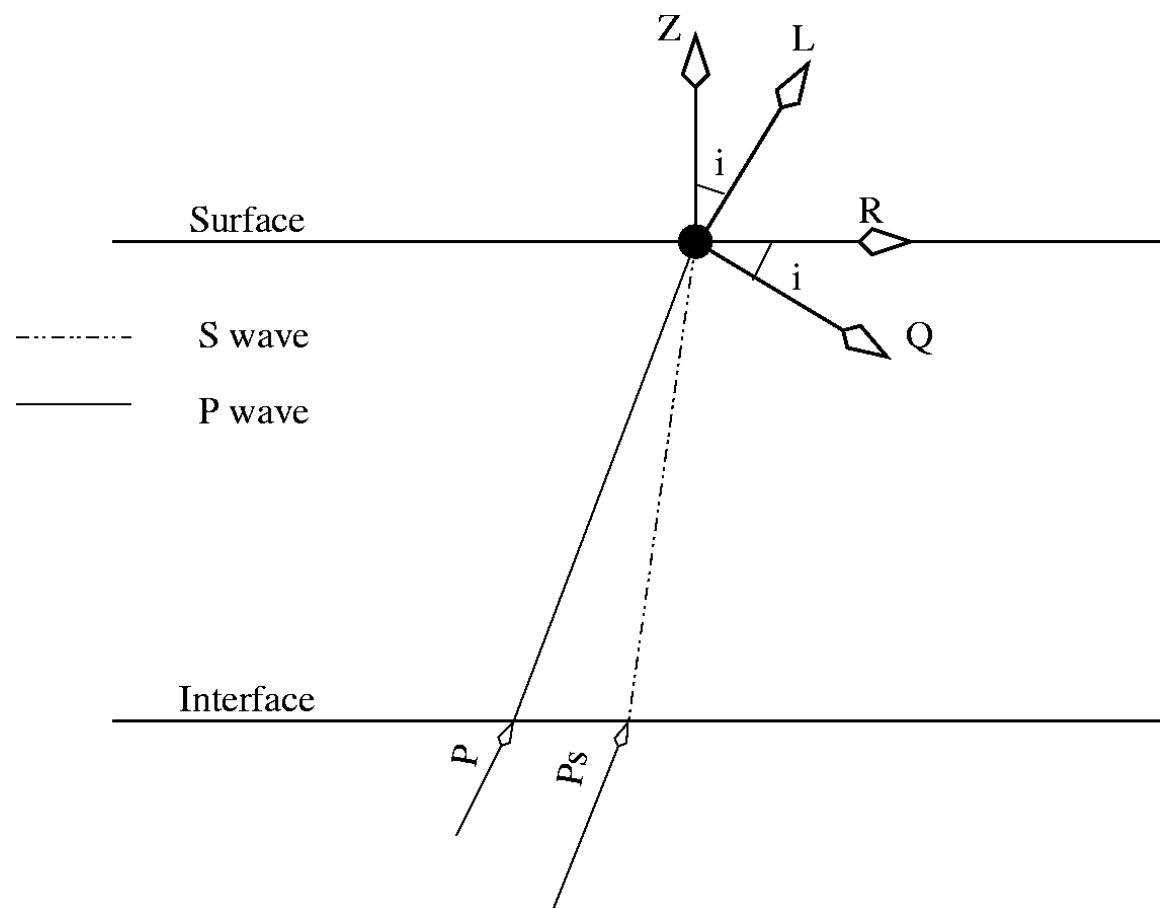


Figure 3.3: Sketch showing the earth-oriented coordinate system Z and R. Labels L and Q represent the axes of the ray coordinate system, L component is in the direction of the incident P wave, Q component is perpendicular to L and points away from the source. T component is perpendicular to both L and Q components.

In case, where the medium is isotropic and the layers are flat (horizontal), the L-component contains mainly the P-energy, Q component contains mainly the SV-energy, and no energy should be seen on the T component. However, anisotropy media and lateral inhomogeneities underneath the seismic station may contribute to energy on the T component.

The rotation can be performed using the theoretical back-azimuth and incidence angle of an incoming P wave. The back-azimuth and incidence angle can be determined by knowing the coordinates of earthquake hypocenter and the recording station for a global velocity model. The alternate way to determine the angles of incidence and back-azimuth is by calculating the eigenvalues of the covariance matrix over a time window spanning the first few seconds following the P-arrival (Kind et al., 1995).

The advantage of using the Q-component instead of the radial component, is the disappearance of projected P-energy at the P arrival time. The first onset marked as (1) on the Q component (Fig. 3.4) is usually the P-to-S conversion from a discontinuity at very shallow depth below the surface.

3.2.3 Deconvolution

In order to calculate the source equalized receiver functions, the deconvolution step was used. (Vinnik, 1977; Phinney, 1964).

Deconvolution of the Q component with P signal on the L component will remove the effects of the source structure and the propagation path effect. The resulting receiver functions (Q component) will contain in the ideal case only the direct conversions and the multiples at discontinuities underneath the recording seismic stations.

Fig. 3.4 is a data example after rotation and deconvolution for one station namely ID08 (see Fig. 4.1 for the location), in which the traces are rotated from the original records into the L, Q and T coordinate system.

The numbers (1) and (2), represents the direct conversions from within the crust and from the Moho, respectively, while number (3) represents the multiple.

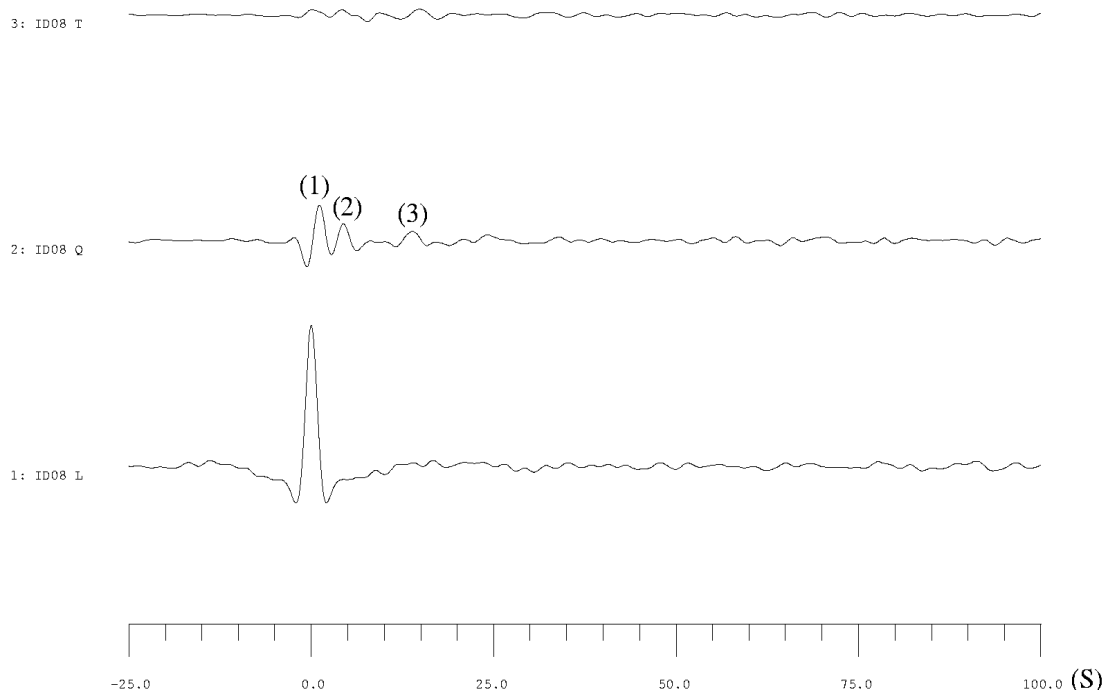


Figure 3.4: A data example for one station (ID08), after rotation of the data into the L, Q and T coordinate system and deconvolution. The L component shows a spike-like waveform. Q component is called receiver function. T component is the tangential receiver function used for the study of anisotropic structures.

Two ways could be used to perform the deconvolution. The first can be performed in time domain, while the second is in the frequency domain. In this study, spiking deconvolution in time domain has been used as described by Kind et al. (1995). Spiking deconvolution is the process of compressing a seismic wavelet, which is the L component into a zero-lag spike. The spiking deconvolution operator is strictly the inverse of the initial segment of the L component (usually 20 seconds following the P onset, which contains most of the P wave energy) that obtained by minimizing the least square differences between the observed seismogram and the desired delta-spike function. This process which is known as least-squares inverse filter is a special case of optimum Wiener filter (Berkhout, 1977).

Then the acquired inverse filter is convolved with the L, Q and T components to obtain the L component or the desired zero-lag spike, source equalized receiver function (Q component) and the deconvolved T components. For each event, all components are normalized to its maximum amplitude on the L component.

In the frequency domain, in terms of spectral division, the observed vertical component which is assumed to consist primarily of unwanted source and path effects is deconvolved from radial component obtained by rotation at the recorded horizontal seismograms. A common implementation for the receiver functions uses the form:

$$F = (HV^*) / (VV^* + w) \quad (3.1)$$

where, F is the Fourier transform of the receiver function, H is the Fourier transform of the horizontal component of the seismogram, V is the Fourier transform of the vertical component of the seismogram, * indicates the complex conjugation, and w is a prewhitening. The prewhitening is carried out by replacing the power level VV^* by water level (Clayton and Wiggins, 1976). The basic problem in the frequency domain is to calculate the Fourier spectra of the radial and horizontal components of the seismogram. For more details see Langston (1979) and Owens et al. (1984).

3.2.4 Moveout Correction

The moveout corrections are dynamically applied to the SV seismograms (Q component) and are predicted accurately by assuming a one dimensional reference model and a constant velocity ratio.

Fig. 3.5 is a simple case of a layer over a half space, that shows the geometry of the Ps conversion generated when the P wave impinges the interface and recorded at seismic station.

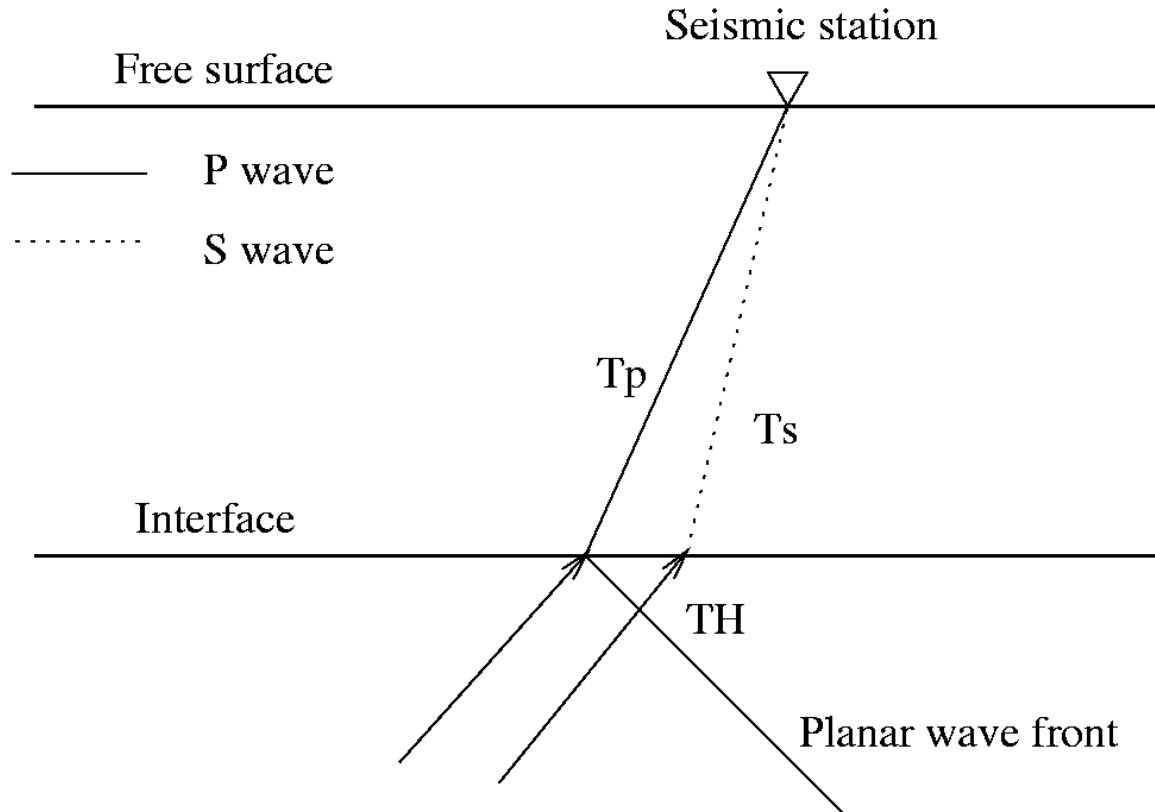


Figure 3.5: Scheme showing the ray paths of direct P and Ps for a layer over a half space. T_p , T_s are the travel times of the P and S phases, respectively. TH is the travel time difference of the two rays in the half space with planar wave approximation.

In receiver function studies with epicentral distances greater than 30° it is acceptable to assume or approximate the incoming P wave as plane wave. The difference in travel time between the conversion and the direct P wave (Ps-P delay time), (Fig. 3.5) is given as:

$$Ps-P(p, H, V_s, V_p) = T_s + TH - T_p \quad (3.2)$$

where p is the ray parameter of the direct P wave, H is the depth of the discontinuity, V_s is the S velocity and V_p is the P velocity in the layer. T_s , TH and T_p are the travel times along the path labeled in Fig. 3.5, (Gurrola et al., 1994). Assuming that the ray parameter for the direct P and the Ps conversions is the same, the delay time of Ps converted wave can be calculated (Kind and Vinnink, 1988) as follow:

$$TPs = H ((Vs^{-2} - p^2)^{1/2} - (Vp^{-2} - p^2)^{1/2}) \quad (3.3)$$

Similarly, delay travel times for crustal reverberations can be given as:

For the PpPs that has two P legs and one S leg is

$$TPpPs = H((Vs^{-2} - p^2)^{1/2} + (Vp^{-2} - p^2)^{1/2}) \quad (3.4)$$

For PpSs and PsPs composed of the sum of reverberations with two S legs and one P leg, and has two contributions with final S leg is

$$TPpSs/PsPs = 2H(Vs^{-2} - p^2)^{1/2} \quad (3.5)$$

Finally, for PsSs that has three S legs is

$$TPsSs = H(3(Vs^{-2} - p^2)^{1/2} + (Vp^{-2} - p^2)^{1/2}) \quad (3.6)$$

The magnitude of the moveout corrections changes with both the depth to the discontinuity and the ray parameter of the incoming P wave. For shallow depth, from the Moho or any other discontinuity in the crust, the variations of the moveout curves are small (usually less than 0.5 seconds), while for deep conversions the variations are large.

The travel times curves for the converted phases in the coda of P wave originating at different depths are not parallel to P. Their slowness decreases for increasing conversion depths. An approach is taken to adjust the times of Ps conversions to what would have been recorded at a certain epicentral distance (67° has been chosen as a fixed distance, that corresponding to ray parameter of $6.4s/^\circ$) according to global one dimensional velocity model (IASP91).

The correction compressed the time scale at receiver functions of shorter distances, while those of the larger than 67° are stretches. So, after the moveout correction, all Ps converted phases should align in parallel to the P wave arrivals, while multiples of the type of PpPs and PpSs are not.

In the upper mantle discontinuities, aligning the moveout corrected receiver functions would help in distinguishing the direct conversions from the multiples.

3.2.5 Inversion

Receiver functions are traditionally inverted to an S wave velocity model that produces an estimation of shear velocity structure under a given seismic station. There is no guarantee that a unique inversion result will be obtained, as the method seeks to minimize the differences between observed and synthetic receiver functions, therefore using a priori information available of the area under investigation will be helpful in constraining the solutions.

The inversion method has been described by Kind et al. (1995). Plane wave theoretical seismograms are computed for the starting model using Haskell's method (1962) for an angle of incidence averaged over all epicentral distances of the recorded receiver functions. The theoretical traces are rotated and deconvolved in the same manner as the observed traces.

The inversion method is a non-linear inversion scheme, which requires an initial velocity depth and then iteratively improves the model by a sequence of relatively thin layers with a gradual increase or decrease of the velocity. For the initial model at a given station, information from reflection/refraction studies were used (DESERT Group, 2003).

The time interval that has been used varies from -5 s prior to the zero phase P wave to 25 s after it. These time intervals include all crustal and upper mantle conversions as well as the strongest multiples.

Fig. 3.6 shows the results of the receiver function inversion for station JS07 (see Fig. 4.1 for the location). Shown are the initial velocity depth model obtained after 4 iterations. The starting velocity depth model (thin lines) and the final model (thick lines), are shown to the left of the corresponding waveform plot after 4 iterations. The uppermost spike-like wave form is the P wave form (L component) obtained after stacking and deconvolution.

The middle and bottom traces depict the observed and stacked waveforms for the starting model (bottom trace) and the final model (middle trace).

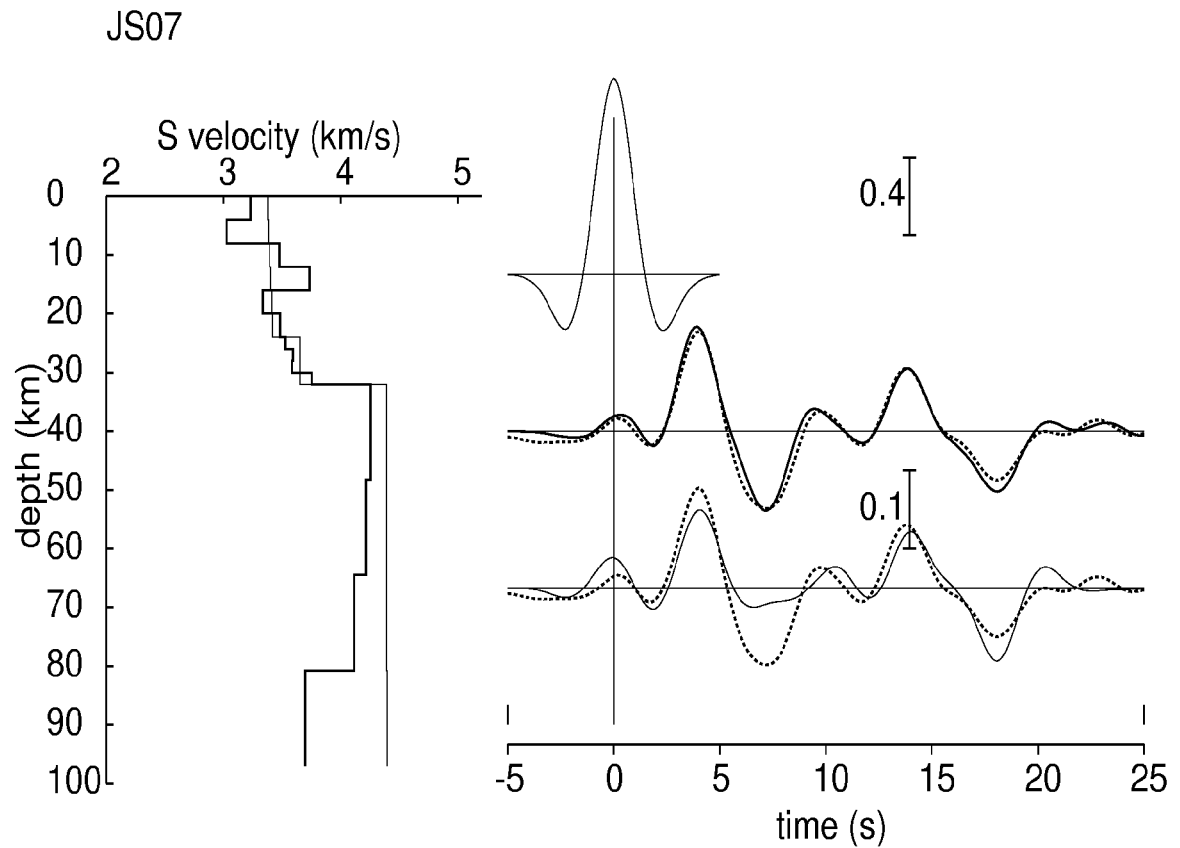


Figure 3.6: Receiver function inversion of station JS07. Starting and final models are shown by thin and thick lines in the left, respectively. The dashed line in the right is the observed receiver function (Q-component), solid lines are synthetic receiver functions for the starting model (thin line at the bottom) and for the final model (thick line of the middle trace) after 4 iterations. The top trace on the right is the input P signal (L-component).

3.2.6 Crustal Thickness and V_p/V_s Estimation

The converted phase Ps and the crustal multiples PpPs and PpSs+PsPs contain a wealth of information concerning the average crustal properties such as the Moho depth and the V_p/V_s ratio.

The delay time of the direct Ps conversion from the Moho and the crustal multiples can be used to estimate the crustal thickness by a given average crustal P velocity. We have used the stacking algorithm proposed by Zhu and Kanamori (2000). This algorithm stacks the amplitudes of receiver functions at the predicted arrival time for the Moho conversion (Ps) and its multiples (PpPs and PpSs+PsPs) for different crustal thicknesses H and Vp/Vs ratios. The advantage of this method is that, there is no need to pick the arrival times of the direct conversion from the Moho and its multiples. Fig. 3.6 shows the relation between crustal thickness and Vp/Vs curves representing the contributions of Ps and the crustal multiples to the stacked amplitudes as a function of crustal thickness and Vp/Vs.

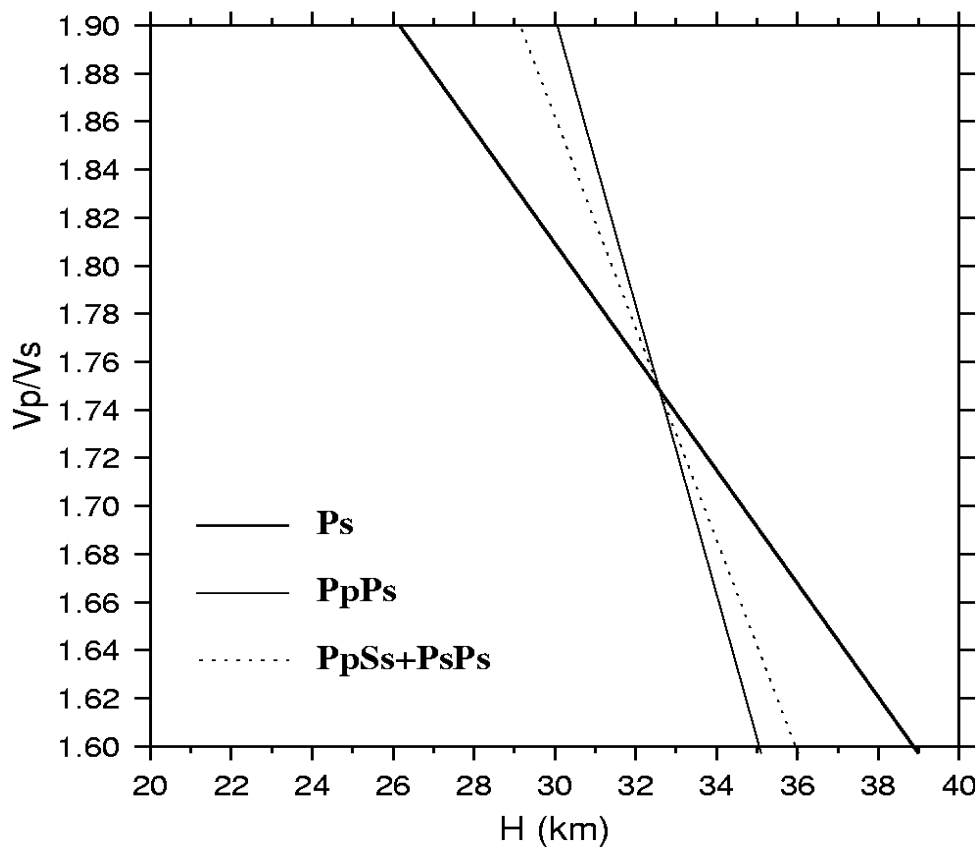


Figure 3.6 : Curves showing the contributions of Ps and its two major crustal multiples (PpPs and PpSs+PsPs) to the stacked amplitude as a function of crustal thickness and Vp/Vs ratio.

Multiple events were used to stack their receiver functions (Q component), in order to increase the signal to noise ratio and the phases are stacked and weighted as follows:

$$S(H, V_p, V_s) = w_1 Q(t_1) + w_2 Q(t_2) - w_3 Q(t_3) \quad (3.7)$$

Where $Q(t_i)$ are the receiver function amplitudes, t_1 , t_2 and t_3 are the predicted travel times for P_s , $P_p P_s$ and $P_p S_s + P_s P_s$ corresponding to crustal thickness H and V_p/V_s ratio, w_i 's are the weighting factors for the direct conversion from the Moho and the multiples. The highest value was given to the direct conversion ($w_1 > w_2 + w_3$), as the slopes of crustal multiples are very similar. The $S(H, V_p, V_s)$ reaches a maximum when all three phases ($P_s, P_p P_s$ and $P_p S_s + P_s P_s$) are stacked coherently.

An example is shown in Fig. 3.7 for one seismic station (ID08) that has clear P_s conversion and crustal multiples. The ray paths are presented at the top.

Consequently, the arrival of the travel times of P_s conversion from the Moho and its multiples were picked at the highest amplitude of the phase which in most cases coincides with the symmetrical center of the phases in order to estimate the crustal thickness using equations 3.3-3-6, and V_p/V_s ratio as follows:

$$V_p/V_s = ((1-p^2 V_p^2)[2(P_s/P_p P_s - P_s) + 1]^2 + p^2 V_p^2)^{1/2} \quad (3.8)$$

Finally, crustal thickness maps and V_p/V_s ratio are produced using both the predicted and the measured arrival times of P_s conversion from the Moho and its multiples.

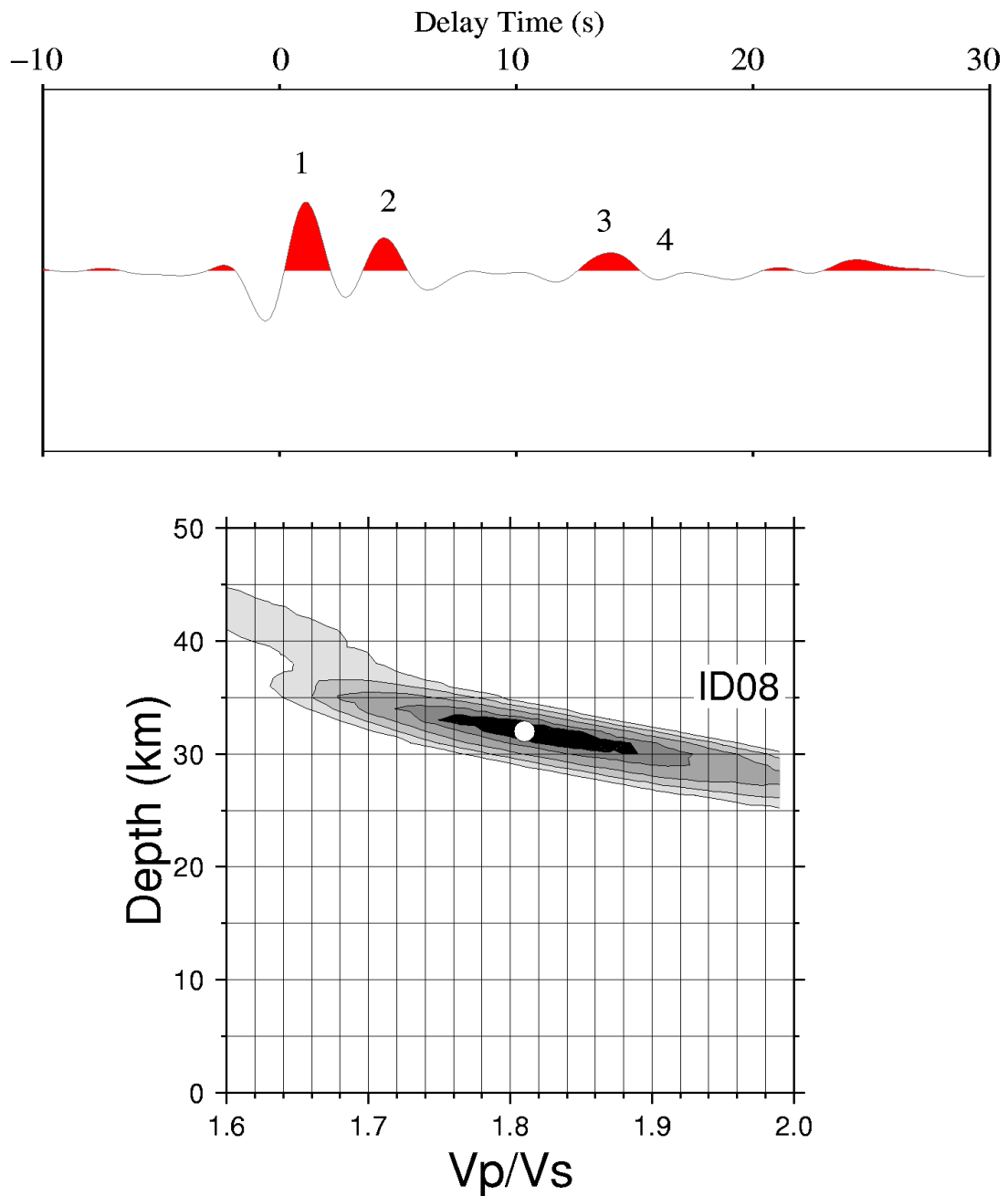


Figure 3.7: A data example to show the application of the Zhu and Kanamori method for one seismic station (ID08), that has clear conversion from the Moho and its crustal multiples. The crustal thickness of 32 km and V_p/V_s ratio of 1.81 are obtained. Labels (1) and (2) at the second panel represent direct conversion within the crust and from the Moho, respectively. (3) and (4) represent the crustal multiples, PpPs and PpSs+PsPs, respectively.